Impact of gravitational force on high repetition rate filamentation of femtosecond laser pulses in the atmosphere

P. Walch, B. Mahieu, L. Arantchouk, Y.-B. André, A. Mysyrowicz, A. Houard

Impact of gravitational force on high repetition rate filamentation of femtosecond laser pulses in the atmosphere

P. Walch,[1] B. Mahieu,[1] L. Arantchouk,[1] Y.-B. André,[1] A. Mysyrowicz,[1] and A. Houard[1,2]
[1)]*Laboratoire d'Optique Appliquée, ENSTA Paris, CNRS, Ecole polytechnique, IP Paris, 91162 Palaiseau, France*
[2)]*Author to whom correspondence should be addressed:aurelien.houard@ensta.fr*

(Dated: 9 April 2024)

We study the influence of the gravitational force on the generation of low-density channels of air left in the path of femtosecond laser filaments at high repetition rate. We observe a more important density variation along the filament longitudinal axis in the case of a vertically created filament as compared to a horizontal one. This leads to a more important reduction of the electrical breakdown field using vertical filament. This geometry induced difference is only observed at high repetition rate because it is directly related to the cumulative effect appearing above 100 Hz.

During the last decade, the development of laser technologies has allowed a new generation of terawatt lasers operating at very high repetition rates[1,2] and a growing attention has been devoted to the consequences of the high repetition rate on various laser induced phenomena such as laser filamentation in air[3–7]. This peculiar nonlinear phenomenon related to the propagation of ultrashort laser pulse with a peak power exceeding a few Gigawatts leads to the creation of a long and homogeneous plasma string in the wake of the laser pulse[8,9], which evolves to form a long-lived under-dense hot gas channel[10,11]. Due to their long lifetime, the creation of consecutive under-dense channels at high repetition rate leads to a cumulative effect[4,12–14] which can greatly increase their efficiency for several applications such as the guiding of electrical discharges[15–19], laser cloud clearing[20,21] or optical air waveguide[22,23]. The same cumulative effect can also have a detrimental effect, by reducing the plasma density[24], or filament length and its emission in the Terahertz domain[25].

While the appearance of the cumulative air density depletion at high repetition rate has already been the object of several studies[4,6,7], a crucial unexplored parameter is the influence of the laser direction, since the buoyant force translates each under-dense channel upward. When the laser propagates horizontally, between each laser shot the buoyant force slightly moves the under-dense channel away from the laser path, resulting in a cumulative channel with a typical asymmetric shape[4]. In this case, provided the repetition rate exceeds 100 Hz, all consecutive channels contribute but do not fully overlap because they are not aligned. By contrast, when the laser propagates vertically, one can expect the buoyant force to move each channel along the direction of the laser path. In this case, each under-dense channel keeps the same alignment and overlap with the previous ones, resulting in a cumulative channel that keeps a circular shape, and has a greater length and a greater density variation. The difference between these two geometries is particularly relevant for atmospheric applications where the beam propagation is mainly vertical, while laboratory experiments are often conducted horizontally.

In this paper, we characterize the cumulative under-dense channel created by a high-repetition rate laser with both vertical and horizontal propagation directions and compare the results to hydrodynamic numerical simulations of the air evolution. We then measure for these two geometries the breakdown voltage reduction produced by the filament and show that the vertical geometry leads to a greater reduction. Finally, we analyze the effect of the laser repetition rate, showing that the dependence to geometry is only present at high repetition rate.

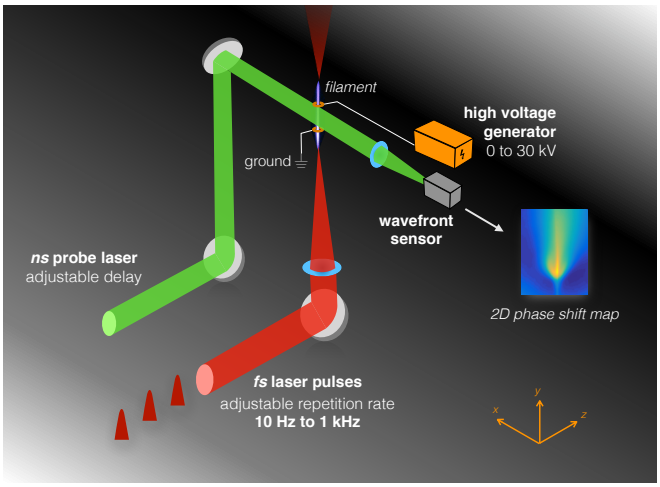

FIG. 1. Experimental setup. A mJ-level femtosecond laser with a repetition rate of 1 kHz, a central wavelength of 800 nm and a pulse duration of 35 fs is focused in air and creates a cm-long filament. The laser propagation is set so that both vertical and horizontal filaments can be created. For both geometries, the resulting low air-density channel is probed by a nanosecond laser beam coupled to a Phasics SID4 wavefront sensor, which records a two-dimensional map of the phase shift induced by the density variation. For discharge guiding measurements, two flat electrodes separated by a distance of 1 cm and pierced in their center to let the filament pass through are placed at different positions along the filament longitudinal axis and connected to a pulsed high-voltage generator.

Using a laser system delivering pulses centered at 800 nm with an energy of 0.8 mJ, a pulse duration of 35 fs at a repetition rate of 1 kHz focused at f/200, we measured using the setup presented in Fig.1 the phase shift linked to the density variation induced by the under-dense channel 100 µs after the last laser pulse for both cases of the laser propagating horizontally and vertically. The 100 µs delay was chosen to ensure

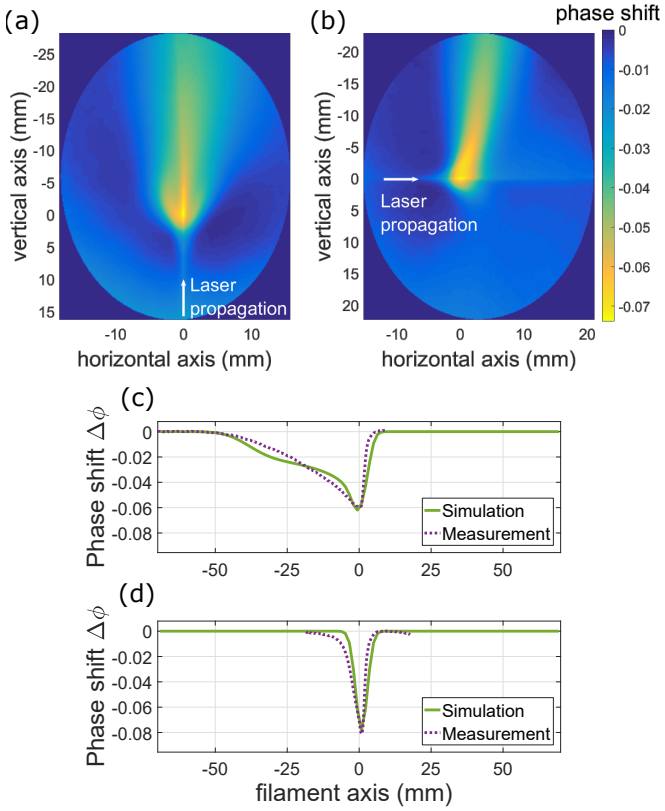

FIG. 2. Phase shift induced by the filamentation of a 1 kHz laser creating 0.8 mJ, 35 fs pulses focused at f/200 in the case of a laser propagating vertically (a) and a laser propagating horizontally (b), measured 100 µs after the last laser pulse and averaged over 100 measurements. Comparison between the measured and simulated phase shift along the filament axis for both a vertical (c) and an horizontal filament (d).

that the system has reached a steady state and that the shockwave generated by the last laser pulse has exited the study area. The result, presented in Fig.2 (a-b), confirms our expectancies: In the case of the laser propagating horizontally, a significant heating is seen away from the filament longitudinal axis due to the buoyant force moving the consecutive channels upward, while the heated zone stays on the filament longitudinal axis in the case of the laser propagating vertically. Consequently, the phase shift, and thus the density reduction, is important over a longer distance in the case of a vertical filament.

To explain the difference between these two geometries, we simulate the air hydrodynamic evolution occurring after each under-dense channel has reached pressure equilibrium with the ambient air at temperature T_{amb}[12]. Due to thermal diffusion, each channel will slowly decay on a millisecond timescale and will move due to the buoyant forces. Using a cartesian coordinate system (x,y,z) defined such as z is the filament longitudinal axis in the case of a horizontal filament and y is the vertical axis, thus corresponding to the filament longitudinal axis in the case of a vertical filament, the temporal temperature evolution of each under-dense channel can be modeled as $T_{horiz/vert}(x,y,z,t) = T_{amb} + \Delta T_{horiz/vert}(x,y,z,t)$ with

$$\Delta T_{horiz}(x,y,z,t) = \Delta T_0 \frac{R_0^2 \times e^{-\frac{x^2+(y-v(t)\times t)^2}{(\sqrt{R_0^2+4\alpha t})^2}}}{(\sqrt{R_0^2+4\alpha t})^2} e^{-\frac{z^2}{(\sqrt{L_0^2+4\alpha t})^2}} \quad (1)$$

$$\Delta T_{vert}(x,y,z,t) = \Delta T_0 \frac{R_0^2 \times e^{-\frac{x^2+z^2}{(\sqrt{R_0^2+4\alpha t})^2}}}{(\sqrt{R_0^2+4\alpha t})^2} e^{-\frac{(y-v(t)\times t)^2}{(\sqrt{L_0^2+4\alpha t})^2}}, \quad (2)$$

where α is the thermal diffusivity of air, ΔT_0 the peak temperature change of the initial Gaussian temperature distribution, R_0 the initial filament radius, L_0 its initial length and $v(t)$ the speed at which the channel moves upward due to the buoyant forces described as

$$v(t) = (1 - \frac{T_{amb} + \Delta T_0}{T_{amb}}) \times g \times t, \quad (3)$$

where g is the acceleration of gravity. Because we can consider that pressure equilibrium is maintained during the studied phase of the temperature evolution, the density and temperature change are linked as

$$\frac{\Delta n}{n_{amb}} = -\frac{\Delta T_{horiz/vert}}{T_{amb}}, \quad (4)$$

where n_{amb} is the ambient air density.

From these expressions, we calculate the phase shift induced by the density variation integrated along the x axis as it measured by our setup, when creating filament at a repetition rate f for both the horizontal and vertical configurations:

$$\Delta\phi_{horiz/vert}(y,z,t) = -\frac{2\pi\beta}{\lambda} \times \sum_{i=0}^{\infty} \int \frac{\Delta T_{horiz/vert}(x,y,z,t+\frac{i}{f})}{T_{amb}} dx, \quad (5)$$

where $\beta = 2.7 \times 10^{-4}$ is the Gladstone-Dale constant, and λ the wavelength of the probe laser[26]. The values used for both L_0 and R_0 are retrieved from experiments conducted at low repetition rate where a single under-dense channel can be characterized and the value of ΔT_0 is chosen as 250 K to best fit our current measurement. The comparison between the simulation of the integrated phase shift along the filament longitudinal axis and the measurement shows a good agreement, as presented in Fig.2 (c-d) and validates our model for both horizontal and vertical geometries. The small discrepancy may arise from the assumption of a gaussian temperature evolution along the filament axis. In reality, while the edges of the filament follow a Gaussian pattern, its central portion appears flatter in terms of temperature distribution.

The reduction of the breakdown voltage produced by a laser filament is mainly due to the reduction of the gas density produced by the filament[27,28]. Because reducing the gas density

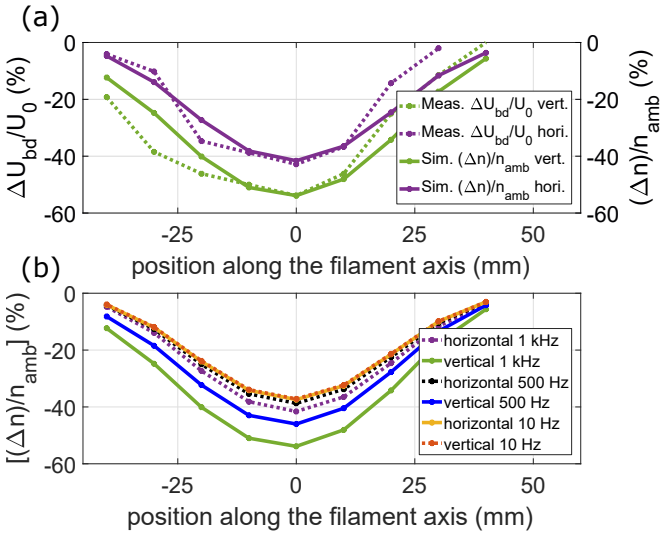

FIG. 3. (a) Comparison between the measured reduction of the breakdown voltage (dashed line) and the mean simulated density variation between the two electrodes (full line), at different positions along the filament longitudinal axis for a vertical (green line) and a horizontal filament (violet line), measured at a laser repetition rate of 1 kHz, with ΔU_{bd} the difference between the measured breakdown voltage in presence of the filament and the natural breakdown voltage U_0. (b) The mean simulated density variation for a repetition rate of 10 Hz, 500 Hz and 1 kHz are presented for both geometries for comparison.

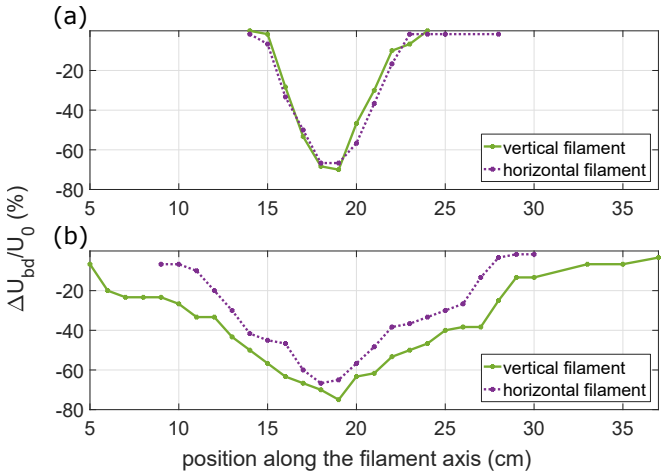

FIG. 4. Measured reduction of the breakdown voltage at different position along the filament longitudinal axis for both a vertical and horizontal axis, measured at (a) 1 Hz and (b) 100 Hz, with U_{bd} the measured breakdown voltage in presence of the filament and U_0 the natural breakdown voltage.

increases the mean free path of the free electrons, the local breakdown field of a Townsend discharge is directly proportional to the gas density. As a consequence a longer and more important density variation along the filament longitudinal axis in the vertical geometry should lead to a greater breakdown voltage reduction over a longer distance. To verify this hypothesis, we added to the setup two flat electrodes separated by a distance of 1 cm and pierced in their center to let the filament pass through. We measured the breakdown voltage between them in the presence of the filament while moving the electrodes along the laser path, to quantify the spatial evolution of the breakdown voltage reduction. These measurements were repeated for both cases of a horizontal and a vertical filament.

The results, presented in Fig.3 (a), show that the reduction of the breakdown voltage is indeed more important in the case of a vertical filament and occur over a longer distance. The maximum reduction reaches 54 % for the vertical filament and only 43 % for the horizontal filament. The full widths at half maximum (FWHM) of the spatial evolution of the breakdown voltage reduction are 5.2 cm and 4 cm for the vertical and horizontal filaments, respectively. If we consider the mean breakdown voltage reduction over the whole filament, an increase of 63 % of the breakdown reduction is measured in the case of a vertical filament.

Using the previously described model, we simulate the mean value of the density variation $\frac{\Delta n}{n_{amb}}$ between the two electrodes along the filament longitudinal axis and compare it to the reduction of the breakdown voltage $\frac{\Delta U_{bd}}{U_{naturalbd}}$ measured at these same positions. The comparison, presented in Fig.3, shows a good agreement between the simulation and the measurement. If we calculate the increase in the integrated reduction of density, an increase of 56 % for the vertical filament compared to the horizontal one is observed, similar to the increase observed in the integrated breakdown reduction. The mean simulated density variation for a repetition rate of 10 Hz and 500 Hz is also presented in Fig.3 (b) showing that this effect of filament orientation is absent at 10 Hz, and progressively increase with the laser repetition rate.

Finally, we analyzed the influence of the laser repetition on this effect. A measurement of the reduction of the breakdown voltage was conducted using a 14 mJ, 50 fs laser pulse focused at f/100 and operating at repetition rates of 1 Hz and 100 Hz. 100 Hz corresponds to the lower repetition rate at which a cumulative effect starts to be observed, while none is present at 1 Hz[4]. The result, presented in Fig.4, shows no difference between the vertical and horizontal configurations for a repetition rate of 1 Hz. This is consistent with our explanation, because no cumulative effect that would create a difference between the two configurations is present in this case. On the contrary, at a repetition rate of 100 Hz the breakdown voltage reduction is larger and more extended in the case of the vertical filament.

In conclusion, we have shown that high repetition rate laser filamentation generates a more important air density depletion when the filaments are created in the vertical direction, as compared to the horizontal direction. This is due to the alignment of the laser propagation axis with the direction of the gravitational force. We have characterized and simulated the induced density depletion as well as the resulting reduction of the breakdown voltage in both geometries, reporting in the vertical configuration an increase of the density depletion and breakdown voltage reduction of 63 % and 56%, respectively.

We also demonstrate that this difference is due to the cumulative effect since it disappears at low laser repetition rate. This effect should play a major role in the efficiency of several applications of filamentation such as the laser lightning rod[19].

ACKNOWLEDGMENTS

The authors acknowledge the European Union Horizon 2020 Research and innovation programme FET-OPEN under Grant No 737033-LLR and the French DGA under Grant No. 2018950901 EPAT3.

DATA AVAILABILITY

The data that support the findings of this study are available from the corresponding author upon reasonable request.

AUTHOR CONTRIBUTIONS

PW, BM, LA, YBA designed and installed the experiment. PW, BM conducted the experiments. PW, BM, AH, AM analyzed the data. PW developed the model and performed the simulations. PW, AH prepared the original draft and all authors critically reviewed and approved the manuscript.

REFERENCES

[1]T. Metzger, A. Schwarz, C. Y. Teisset, D. Sutter, A. Killi, R. Kienberger, and F. Krausz, "High- repetition-rate picosecond pump laser based on a yb:yag disk amplifier for optical parametric amplification," Opt. Lett **34**, 2123–2125 (2009).

[2]C. Herkommer, P. Krotz, R. Jung, S. Klingebiel, C. Wandt, R. Bessing, P. Walch, T. Produit, K. Michel, D. Bauer, R. Kienberger, and T. Metzger, "Ultrafast thin-disk multipass amplifier with 720 mj operating at kilohertz repetition rate for applications in atmospheric research," Opt. Express **28**, 30164 (2020).

[3]A. Houard, V. Jukna, G. Point, Y.-B. Andre, S. Klingebiel, M. Schultze, K. Michel, T. Metzger, and A. Mysyrowicz, "Study of filamentation with a high power high repetition rate ps laser at 1.03 μm," Opt. Express. **24**, 7437–7448 (2016).

[4]P. Walch, B. Mahieu, L. Arantchouk, Y.-B. Andre, A. Mysyrowicz, and A. Houard, "Cumulative air density depletion during high repetition rate filamentation of femtosecond laser pulses: Application to electric discharge triggering," Appl. Phys. Lett. **119**, 264101 (2021).

[5]P. Walch, B. Mahieu, V. Moreno, T. Produit, U. Andral, Y.-B. André, L. Bizet, M. Lozano, C. Herkommer, M. Moret, R. Jung, R. Bessing, S. Klingebiel, Y. Bertho, T. Metzger, A. Mysyrowicz, J.-P. Wolf, J. Kasparian, and A. Houard, "Long distance laser filamentation using yb:yag khz laser," Sci. Rep. **13**, 18542 (2023).

[6]T.-J. Wang, M. H. Ebrahim, I. Afxenti, D. Adamou, A. C. Dada, R. Li, Y. Leng, J.-C. Diels, D. Faccio, A. Couairon, C. Milián, and M. Clerici, "Cumulative effects in 100 khz repetition-rate laser-induced plasma filaments in air," Adv. Photonics Res. **4(3)**, 2200338 (2023).

[7]R. Loscher, V. Moreno, D. Adamou, D. K. Kesim, M. C. Schroeder, M. Clerici, J.-P. Wolf, and C. J. Saraceno, "High-power sub-picosecond filamentation at 1.03 µm with high repetition rates between 10 and 100 khz," APL Photonics **8**, 111303 (2023).

[8]A. Couairon and A. Mysyrowicz, "Femtosecond filamentation in transparent media," Phys. Rep. **441**, 47–189 (2007).

[9]J.-C. Diels, *Light Filaments: Structures, Challenges and Applications* (Scitech Publishing, 2021).

[10]G. Point, C. Milian, A. Couairon, A. Mysyrowicz, and A. Houard, "Generation of long-lived underdense channels using femtosecond filamentation in air," J. Phys. B. **48**, 094009 (2015).

[11]Y.-H. Cheng, J. K. Wahlstrand, N. Jhajj, and H. M. Milchberg, "The effect of long timescale gas dynamics on femtosecond filamentation," Opt. Express **21**, 4740–4751 (2013).

[12]J. K. Wahlstrand, N. Jhajj, and H. M. Milchberg, "Controlling femtosecond filament propagation using externally driven gas motion," Opt. Lett. **44 (2)**, 199–202 (2019).

[13]A. Higginson, Y. Wang, H. Chi, A. Goffin, I. Larkin, H. M. Milchberg, and J. J. Rocca, "Wake dynamics of air filaments generated by high-energy picosecond laser pulses at 1 khz repetition rate," Opt. Lett. **46**, 5449–5452 (2021).

[14]F. Yin, J. Long, Y. Liu, Y. Wei, B. Zhu, K. Zhou, T.-J. Wang, Y. Leng, and R. Li, "Pulse repetition-rate effect on the intensity inside a femtosecond laser filament in air," High Power Laser Science and Engineering **11**, e46 (2023).

[15]F. Théberge, J.-F. Daigle, J.-C. Kieffer, F. Vidal, and M. Châteauneuf, "Laser-guided energetic discharges over large air gaps by electric-field enhanced plasma filaments," Sci. Rep. **7**, 40063 (2017).

[16]O. G. Kosareva, D. V. Mokrousova, N. A. Panov, I. A. Nikolaeva, D. E. Shipilo, E. V. Mitina, A. V. Koribut, G. E. Rizaev, A. Couairon, A. Houard, A. B. Savel'Ev, L. V. Seleznev, A. A. Ionin, and S. L. Chin, "Remote triggering of air-gap discharge by a femtosecond laser filament and postfilament at distances up to 80 m," Appl. Phys. Lett. **119 (4)**, 041103 (2021).

[17]L. Arantchouk, G. Point, Y. Brelet, B. Prade, J. Carbonnel, Y.-B. Andre, A. Mysyrowicz, and A. Houard, "Large scale tesla coil guided discharges initiated by femtosecond laser filamentation in air," J. Appl. Phys. **116**, 013303 (2014).

[18]Z. Pei, W. Chen, X. Fan, J. Gu, S. Huang, X. Liu, Z. Fu, B. Du, T. Wang, R. Zhang, and Q. Zhang, "The contribution of femtosecond laser filaments to positive and negative breakdown discharge in a long air gap," Physics of Plasmas **30**, 043511 (2023).

[19]A. Houard, P. Walch, T. Produit, V. Moreno, B. Mahieu, A. Sunjerga, C. Herkommer, A. Mostajabi, U. Andral, Y.-B. Andre, M. Lozano, L. Bizet, M. C. Schroeder, G. Schimmel, M. Moret, M. Stanley, W. A. Rison, O. Maurice, B. Esmiller, K. Michel, W. Haas, T. Metzger, M. Rubinstein, F. Rachidi, V. Cooray, A. Mysyrowicz, J. Kasparian, and J.-P. Wolf, "Laser-guided lightning," Nat. Photonics **17**, 231–235 (2023).

[20]G. Schimmel, T. Produit, D. Mongin, J. Kasparian, and J.-P. Wolf, "Free space laser telecommunication through fog," Optica **5 (10)**, 1338 (2018).

[21]A. Goffin, J. Griff-McMahon, I. Larkin, and H. Milchberg, "Atmospheric aerosol clearing by femtosecond filaments," Phys. Rev. Appl. **18**, 014017 (2022).

[22]S. Fu, B. Mahieu, A. Mysyrowicz, and A. Houard, "Femtosecond filamentation of optical vortices for the generation of optical air waveguides," Opt. Lett. **47**, 5228 (2022).

[23]A. Goffin, I. Larkin, A. Tartaro, A. Schweinsberg, A. Valenzuela, E. W. Rosenthal, and H. M. Milchberg, "Optical guiding in 50-meter-scale air waveguides," Phys. Rev. X **13**, 011006 (2023).

[24]F. Yin, T.-J. Wang, Y. Liu, J. Long, Y. Wei, B. Zhu, K. Zhou, and Y. Leng, "Pulse repetition rate effect on the plasma inside femtosecond laser filament in air," Chin. Opt. Lett. **22**, 013201 (2024).

[25]A. D. Koulouklidis, C. Lanara, C. Daskalaki, V. Y. Fedorov, and S. Tzortzakis, "Impact of gas dynamics on laser filamentation thz sources at high repetition rates," Opt. Lett. **45**, 6835–6838 (2020).

[26]G. Point, Y. Brelet, L. Arantchouk, J. Carbonnel, B. Prade, A. Mysyrowicz, and A. Houard, "Two-color interferometer for the study of laser filamentation triggered electric discharges in air," Rev. Sci. Instrum. **85 (12)**, 123101 (2014).

[27]Y. P. Raizer, *Gas discharge physics* (Springer, 1991).

[28]S. Tzortzakis, B. Prade, M. Franco, A. Mysyrowicz, S. Huller, and P. Mora, "Femtosecond laser-guided electric discharge in air," Phys. Rev. E **64**, 057401 (2001).